Magnetically Accelerated Plasmoid (MAP) Thruster - Initial Results and Future Plans

IEPC-2007-16

Presented at the 30th International Electric Propulsion Conference, Florence, Italy
September 17-20, 2007

John Slough*, Arthur Blair, Chris Pihl, and George Votroubek.
MSNW, Redmond, WA 98052, USA

Abstract: The dynamic formation of a self confined plasmoid known as the field reversed configuration, and the subsequent acceleration by magnetic forces has been demonstrated in the Magnetically Accelerated Plasmoid (MAP) experiments. A methodology for repetitive operation was identified and demonstrated. The ejection velocity was at least 180 km/s for each plasmoid giving a total impulse bit of 0.3 N-s. The CW operation of a MAP thruster would thus provide a jet power up to 75 MW. For near term applications, a lower power, lower Isp thruster is desired. Towards that end, an electrodeless RF plasmoid formation system based on rotating magnetic fields has been constructed and demonstrated. An optimization study of this plasmoid source coupled to the MAP thruster was performed with a projected thruster efficiency of 70-80% with an Isp of 6 to 8 ksec. The practical implementation of this thruster can be achieved with current solid state switching technology. The prototype thruster is currently being constructed and the initial thruster electrical design and testing was performed achieving sufficiently high efficiency (> 90%).

Nomenclature

B_z	=	Magnitude of axial magnetic field
B_{vac}	=	Vacuum magnetic field magnitude
B_{RMF}	=	Magnitude of rotating magnetic field
B_{ext}	=	Magnetic field radially external to the FRC
B_φ	=	FRC internal flux divided by coil area$_l$
β	=	Ratio of plasma to magnetic field energy density i.e. $nkT/(B^2/2\mu_0)$
δ	=	Classical skin depth in a conductor
ε_B	=	Magnetic energy coupling coefficient
E_{conv}	=	Energy lost from particle convection
E_d	=	FRC directed energy
E_{ff}	=	Frozen flow energy loss
E_i	=	Energy required for ionization
E_{Loss}	=	All thruster plasma energy losses other than E_i and E_d
R_{rad}	=	Energy loss from plasma radiation
E_θ	=	Azimuthal component of the induced electric field
E_B	=	Magnetic energy inside accelerator coils
ELF	=	Electrodeless Lorentz Force thruster
FRC	=	Field Reversed Configuration
φ_i	=	FRC internal closed (poloidal) flux

φ_{ext} = Axial flux external to FRC
F_z = Thrust in axial (z) direction
η_{PPU} = Efficiency of PPU
η_{tot} = Total thruster efficiency
η_{th} = Thruster efficiency
η_{ee} = Effective electrical efficiency of PPU
Isp = Specific impulse
I_θ = Total driven azimuthal current
j_θ = Azimuthal current density
j = Current density
K_L = Solenoid finite length correction coefficient
K = Rigid rotor parametric coefficient
KE = Directed kinetic energy of FRC plasmoid
L = Coil inductance
L_{ac} = Accelerator length
l_s = FRC length
m_d = Dipole moment of induced FRC diamagnetic current
m_i = Mass of plasma ion
M = Mass of FRC
MAP = Magnetically Accelerated Plasmoid
MHD = Magneto-Hydrodynamics
MPD = Magneto-Plasmadynamic
μ_0 = Magnetic permeability
ν_{ei} = electron-ion collision frequency
N = Particle inventory of FRC
n_e = plasma electron density (meters^{-3})
PIT = Pulsed Inductive Thruster
PPU = Power Processing Unit
RMF = Rotating Magnetic Field
RR = Rigid Rotor equilibrium profile
r = Radial distance in cylindrical coordinates
r_c = Coil radius
r_s = Separatrix radius of FRC
T = FRC plasma total temperature
P_{RMF} = Power delivered into plasma by RMF antenna
τ_N = Particle confinement time
T_e = Electron temperature in eV
v_z = FRC axial velocity
ω_{RMF} = rotation frequency of the rotating magnetic field
ω_{ce} = electron cyclotron frequency in the rotating magnetic field B_{RMF}
ω_{ci} = the ion cyclotron frequency
x_s = ratio of separatrix to coil radius
Z = Reactive impedance

I. Introduction

THE production of a field reversed configuration (FRC) plasmoid and subsequent acceleration by magnetic forces is a promising approach to high-thrust and high performance space propulsion. A research facility was designed to demonstrate this potential, determine optimal performance, and examine the technology required to move toward the design of practical high-performance space propulsion system. The Magnetically Accelerated Plasmoid (MAP) experiment was designed to produce a compact toroidal plasmoid commonly referred to as a Field Reversed Configuration[1] (FRC) and accelerate it to high velocity using a sequenced set of coils. The MAP thruster was adjoined to a drift tube to better characterize the performance (see Fig. 1). Having achieved the first step of

demonstrating thruster operation, the current activity has been directed toward determining the optimal performance and maturation of the technology towards the design of practical high-performance space propulsion system. The paper will discuss these efforts as well as the results and analysis based on the first set of experiments.

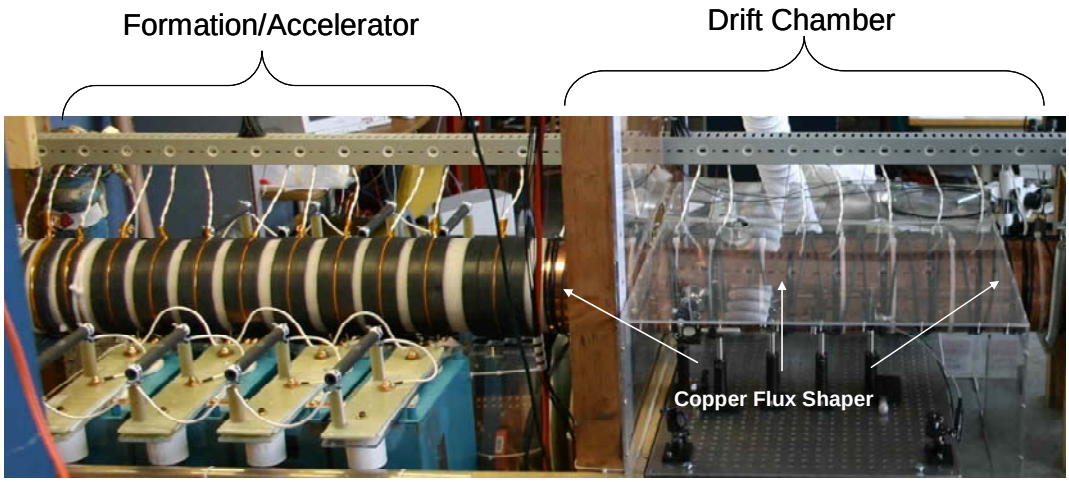

Figure 1. Magnetically Accelerated Plasmoid (MAP) thruster experiment.

An analytical treatment of the acceleration process was performed and a set of 2D MHD calculations were conducted[2]. Both the analytical model as well as the numerical calculations were compared and validated with the experimental measurements, and the initial results of these efforts are reported elsewhere[3]. Details of the formation and acceleration of the FRC plasmoid and the performance of various ancillary systems required for successful formation were also outlined. A novel and efficient method for producing and accelerating the FRC plasmoid was developed, and is referred to as dynamic formation. A plot of the plasmoid motion during dynamic formation and acceleration in single pulse operation is found in the Fig. 2.

With dynamic formation a method for producing a quasi-continuous (CW), high efficiency thruster was also developed and demonstrated. It was possible for the first time to produce sequentially a series of FRC plasmoids. The formation and acceleration of these FRCs was accomplished by operating the set of eight coils in a manner that produced a traveling magnetic wave for several cycles. The MAP thruster in this mode of operation produced plasmoids at high Isp (~ 18 ksec) and demonstrated operation at very high peak power (70 MW).

The repetitive generation of FRC plasmoids is a requisite for the implementation of MAP as a thruster. Lower power operation at lower Isp is also an important experimental goal. Operation in a repetitive pulse mode has been explored in a limited way in prior efforts[4], and will be extended and employed in the next phase of experiments. Another promising mode of operation has recently been explored experimentally. This method of plasmoid formation employs a rotating magnetic field[5] (RMF). It is an electrodeless process where the necessary plasma currents are driven non-inductively through the Hall effect. The device can form plasmoids with high mass propellants at high thrust. The MAP accelerator coils would then be mated to the output of the formation coil to increase the axial energy and thus the efficiency of the thruster. Analysis of the expected efficiency of the MAP thruster was performed for the repetitive mode of operation employing the RMF startup with various propellant options The critical issues for this mode of operation are outlined in the next section. The final section discusses the prototype thruster under construction with the focus being the technological achievements that must be accomplished for a working thruster to be realized.

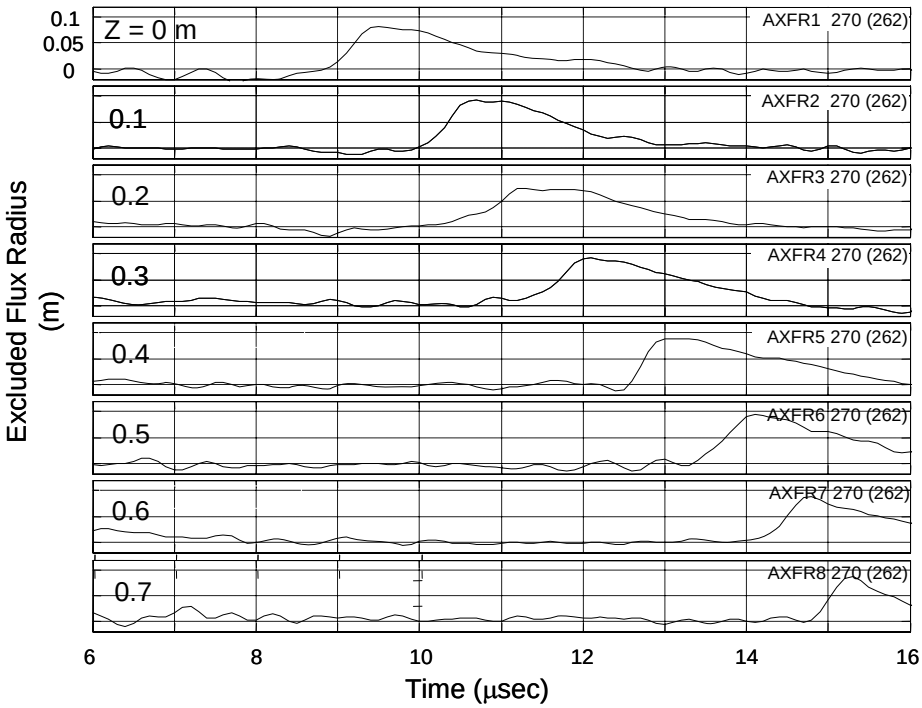

Figure 2. Plasmoid Exluded Flux Radius in MAP accelerator. *Traces are for acceleration using coil timing for optimum exit velocity of the FRC.*

II. MAP Thruster Optimization

A. Determination of the Optimum Scale for MAP

A critical decision for obtaining the optimum performance of a plasmoid based thruster is the choice for the scale of the device. There are several factors that must be taken into consideration. Clearly the most essential are those factors that govern the physical processes involved in the formation and acceleration of the FRC plasmoid. Second to these is the dependence of various loss mechanisms on the physical parameters of the plasmoid such the plasmoid size, density, temperature, and ionic composition. Finally there are the constraints imposed by the technology that is employed to repetitively produce, accelerate and eject the FRC plasmoid. In short then the three main factors to be considered are: *(1) FRC plasmoid production, acceleration, ejection physics (2) Transport, radiation, and conduction loss scaling (3) PPU efficiency and energy transfer effectiveness.* All three are coupled to differing degrees, and will have differing optimums. Even these optimums are likely to change as target thrust, Isp and efficiencies are varied. Designing a prototype MAP thruster configuration thus becomes a rather daunting challenge.

A good starting point for simplification is to restrict the range by choosing a target jet power, thrust, and Isp based on mission requirements. Clearly these are not independent selections, but the flexibility provided by a pulsed device allows for the pulse rate, and thus jet power to vary independently from the impulse bit, and specific impulse. The target goal of the prototype MAP thruster will be 10 MW of average jet power, at an Isp of 5 to 10 ksec, and a thrust of 200 - 400 N.

Efficiency must always be the overriding factor in any discussion of thruster design. Typical efficiencies of high power thrusters such as the MagnetoPlasmaDynamic (MPD)[6] and Pulsed Inductive Thruster (PIT)[7] are in the 50% range. As the power increases it becomes even more imperative to have the efficiency be as high as possible as the waste heat must be handled by a separate radiator whose mass will increase with rejected power. For a thruster with efficiency η, the waste heat will scale as $1-\eta$. The ratio of radiator mass-to thruster mass will thus scale as $(1-\eta)/\eta$ as depicted in Fig. 3. It is clear from this figure, if one wishes the thruster specific power to be dominated by the thruster system mass and not the radiator, efficiencies of 70% or better would be desirable.

Considering the typical operating regimes of most FRC plasmoid experiments, an immediate concern is not achieving the target parameters in a single or short burst of pulses. This has been already demonstrated in the initial MAP thruster experiments. The second consideration is also not of paramount urgency. The FRC is magnetically isolated and has a confinement that is typically much longer than the residence time in the thruster. It is the final consideration that becomes the tail that wags the dog, so to speak. The requirement for efficient, repetitive plasmoid formation/acceleration demands a change in the way the typical FRC plasmoid has been produced in the past. Dependence on simple spark gap or thyratron switched capacitors at high voltage leads to significant PPU inefficiencies. Fortunately it is possible to find devices that can function in this role, but it does require a significant change in operation over and above the obvious one of repetitive formation. The power transfer employed in the field reversed theta pinch formation employing high voltage (> 10 kV) capacitor switching is in the gigawatt range. By employing a low duty cycle (100s of Hz), one can reduce the average jet power into the target range, but it would be prohibitive to try to simply replace the switches with solid state devices.

In recent experiments on the Electrodeless Lorentz Force[8] (ELF) thruster a rotating magnetic field (RMF) was employed to generate the plasmoid diamagnetic currents rather than rapid field reversal. This plasmoid, coupled to a MAP type accelerator, could thus potentially provide a means to form the FRC and accelerate it without having to resort to the inefficient high voltage, high power technology employed in past experiments. Assuming that one can start the FRC with RMF, and finish with a MAP thruster based on solid state switching, the question of scale now is determined primarily by aspects of factor (1). The other factors represented in (2) are generic and would be considered after an optimum size scale has been determined. Again, there is however one overriding consideration. High efficiency (> 60%) will no doubt require the use of a propellant with a mass significantly greater than a hydrogenic one given the relatively low target value of Isp (initial MAP results had Isp ~ 20 ksec for D_2). Radiation and ionization losses could be a factor at the typical FRC density (~ 10^{21} m^{-3}) so that the target FRC density should be significantly lower (although the FRC total mass can and will be higher).

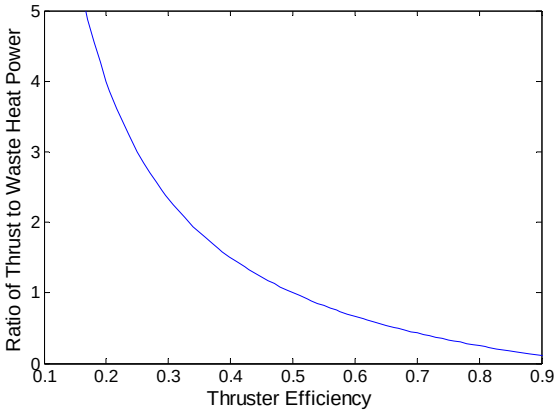

Figure 3. Thruster efficiency effect on system power (mass).

The RMF formation is quite compatible with this, and results from the ELF thruster were as good in Argon as Deuterium. What this implies, together with the confinement scaling observed in past experiments, is that bigger is generally better. How big is the question. All three factors will constrain the answer to some extent. The first constraint to be considered comes in the form of accelerator power coupling. For this determination, a brief review of the dependence of the FRC kinetic energy on accelerator parameters will be given.

Optimum parameters from MAP physics

During the compression and acceleration of the FRC in MAP, the changing magnetic field induces image currents within the FRC as the FRC acts like a perfectly conducting medium on these short timescales. The force on the diamagnetic current loop induced by the changing external magnetic field is given by:

$$\mathbf{F} = \mathrm{M}\frac{\mathrm{d}\,\mathbf{v}}{\mathrm{d}\,\mathrm{t}} = \nabla(\mathbf{m}_{\mathrm{d}} \cdot \mathbf{B}) \tag{1}$$

where dipole moment, $\mathbf{m}_{\mathrm{d}}$, is the magnetic dipole moment from the induced currents in the FRC of mass M.

It is possible to get an approximate expression for the dipole moment by considering the much simpler case of a conductor in a homogeneous axial magnetic field. The magnetic scalar potential for a spherical conductor can be readily obtained from Laplace's equation. The solution for a perfectly conducting diamagnetic sphere (magnetic field separatrix coincident with sphere surface) in a homogeneous field, B_{vac} is:

$$\phi_M = \frac{B_{vac}}{\mu_0} z\left(1 + \frac{r_s^3}{2(r^2 + z^2)^{3/2}}\right) \tag{2}$$

where r_s is the sphere radius. The first term corresponds to the potential of the homogeneous field. The second corresponds to that of a dipole parallel to the z axis with a moment:

$$\mathbf{m}_d = -\tfrac{1}{2} r_s^3 \frac{\mathbf{B}_{vac}}{\mu_0} \tag{3}$$

With the purely axial nature of the magnetic moment, the axial component of the magnetic force from Eq. (1) can be reduced to:

$$F_z = m_d \cdot \nabla B_z = m_d \frac{\partial B_z}{\partial z} \tag{4}$$

There is no net axial force on the FRC, regardless of shape, in a homogeneous field. The force from the +z side is countered by the force from the –z side. If one assumes the ideal driving magnetic waveform, where there is magnetic field only on the upstream half of the FRC, the maximum force will derived. The approximation that the shape of the end of the FRC residing in the driving coil being hemi-spherical is a reasonable enough based on the numerical calculations. Changes in shape from other than hemi-spherical will change slightly the numerical coefficient for m_d given in Eq. (3), but the basic scaling will be the same. The approximation that the downstream field be negligible compared to the driving field should also be close to what can be achieved in the actual thruster.

What is left is to determine the dependence on the FRC separatrix radius as a function of the driving field. This depends somewhat on the internal magnetic profile. The profile that most closely fits the FRC equilibrium measurements is that generally referred to as the rigid rotor (RR) profile where $J_\theta(r) = n(r)e\omega r$. In this case, the closed poloidal flux, φ_i, is given by the following expression:

$$\varphi_i = \frac{\pi}{2\sqrt{2}} \frac{B_{ext}}{r_c} r_s^3 \tag{5}$$

The magnitude of the dipole moment of the FRC can now be stated in terms of the trapped poloidal flux inside the FRC:

$$m_d = \frac{\sqrt{2}}{\pi} r_c \varphi_i (1 - x_s^2) \tag{6}$$

where flux conservation within the cylinder was invoked i.e. $B_{ext} = B_{vac}/(1-x_s^2)$

The axial gradient scale length has as a practical minimum, - that given by the length over which the external coils can generate a large ΔB change between them. The minimum is certainly on the order of $\Delta z \sim 2r_c$. Assuming this minimum, one has from Eq. (4):

$$F_z \sim m_d \frac{\Delta B_z}{\mu_0 \Delta z} = \frac{\sqrt{2}}{2\pi} \varphi_i \frac{B_{vac}}{\mu_0} \tag{7}$$

The work done by the accelerator fields on the FRC in traveling a distance d along the accelerator is $F_z \cdot d$, and is ideally equal to the kinetic energy acquired by the FRC. The total kinetic energy acquired from an accelerator of length L_{ac} is then:

$$KE = \tfrac{1}{2} M v_z^2 = \frac{\sqrt{2}}{2\pi} L_{ac} \varphi_i \frac{B_{vac}}{\mu_0} \tag{8}$$

One can define B_φ as the FRC flux normalized to the coil area, i.e.

$$B_\varphi \equiv \frac{\varphi_i}{\pi r_c^2} \cong 0.05. \tag{9}$$

As stated in Eq. (9), a fairly constant maximum value for B_φ is observed over a wide range of FRC experiments with only a weak dependence fill pressure. It should be noted that in the dynamic formation experiments on MAP, this value can be significantly increased due to the near simultaneous field reversal and ejection of the FRC from coil to coil. For the purposes here the fixed value derived from past experiments will suffice as B_φ is not expected to vary with size with dynamic formation any differently than in standard *in situ* formation.

The recent work on the ELF thruster with RMF startup, a wholly different set of parameters could determine the poloidal flux that can be generated in the FRC. The discussion must thus take two paths. The one to be considered here will be that of field-reversed dynamic formation as that was the method successfully employed in the MAP thruster experiments. The other will be determined in efforts on the ELF experiment at MSNW. Using the empirical result stated in Eq. (9) in Eq. (8) one obtains:

$$KE = \frac{\sqrt{2}}{\pi}\frac{B_\varphi}{B_{vac}} E_B \tag{10}$$

where E_B is the sum of all the vacuum magnetic energy that was introduced inside a coil of radius r_c and length L_{ac} during dynamic formation and the subsequent acceleration. It can be seen that the kinetic energy scales only with the magnetic energy introduced into the system during the process of acceleration. Since B_φ is a relatively fixed parameter, it would appear from Eq. (10) that for a given bank energy, one would want to minimize the vacuum magnetic field to maximize coupling efficiency. While this seems counter intuitive, it is really just a reflection of the fact that at constant bank energy, increasing the accelerator length is preferable to increasing the field (see Eq. 8) as that dependence is linear rather than the square root. There is a limit as to how small a ratio of B_φ to B_{vac} is practical. The separatrix radius is a function of this ratio. For most FRC experiments the internal field profile is consistent with the azimuthal electron drift being constant. For the formation of the FRC by a rotating magnetic field as in the ELF experiments, it is fixed at the rotation frequency.

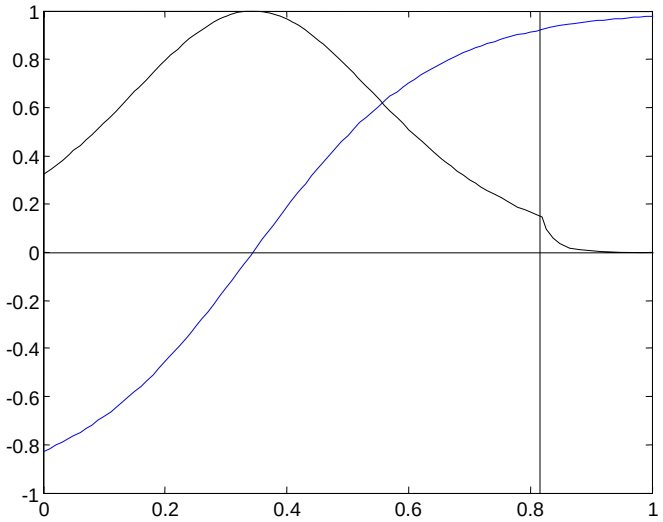

Figure 4. Normalized axial magnetic field (blue line) and density for RR profile with x_s = 0.83. *The FRC density is truncated at the separatrix (indicated by vertical line) by plasma loss on the external field.*

As was mentioned, the profile is referred to as a rigid rotor (RR). The RR profile (see Fig. 4) is defined by

$$B(r) = B_{ext} \tanh K\left(\left(\frac{r}{R}\right)^2 - 1\right) \tag{11}$$

where R is the radius of the field null within the FRC. It is related to the separatrix radius, $r_s = \sqrt{2}\,R$. This relation is quite general as it reflects the geometric area ratio of inner to outer closed flux within the FRC regardless of profile. The variable κ that characterizes the rigid rotor is constrained by what is referred to as the average β constraint: $\langle\beta\rangle = (1 - \tfrac{1}{2} x_s^2)$. This constraint can be derived from the FRC being in axial pressure balance with the external magnetic field. One can show that[1]:

$$\frac{\tanh K}{K} = 1 - \frac{1}{2}x_s^2 \tag{12}$$

The sequential excitation of the axial array of coils in MAP has a varying axial flux all along the coil set. This certainly complicates the simple relation that is commonly used to describe this constraint in the typical FRC

formation where the flux is constant along a single monolithic coil. Even though the flux varies from coil to coil, the expression in Eq. (12) can still be used as it reflects the (axially) local radial profile observed in the 2D MHD calculations for the quasi-steady dynamic acceleration of the FRC plasmoid.

The ratio of the inner to external flux for the RR can be stated as

$$\frac{\varphi_i}{\varphi_{ext}} = \frac{x_s^2}{2}\frac{\ln\cosh(K)}{K} \tag{13}$$

Over the range of interest κ can be closely approximated as $K = \sqrt{2}\, x_s$. Relating the external flux to the vacuum field assuming flux conservation, one has for the ratio of normalized trapped flux to vacuum field:

$$\frac{B_\varphi}{B_{vac}} \cong \frac{\sqrt{3/2}}{4}\frac{x_s^3}{1-x_s^2} \tag{14}$$

A plot of this ratio as a function of the separatrix to coil radius ratio, x_s, is shown in Fig. 5. As can be seen, a large ratio can only be obtained at very large x_s. This is somewhat divergent to maintaining the FRC sufficiently far from the thruster wall to eliminate conduction losses. Clearly, experiment should be the best method for determining the maximum x_s, and that will certainly be part of the future effort on MAP. For the scoping study a value of ~ 0.5 for the flux ratio will be assumed ($x_s \sim 0.83$) as that was typical of the leading end of the FRC plasmoids formed in the MAP experiments. The RR profiles for this value are what were plotted in Fig. 4.

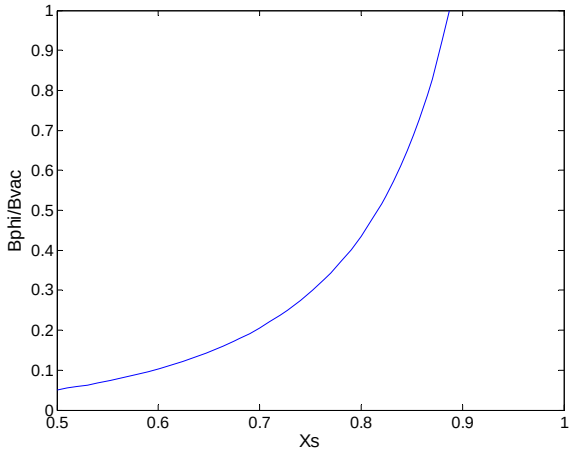

Figure 5. Normalized FRC internal flux to vacuum flux ratio as a function of FRC separatrix to coil ratio

In the process of acceleration, the upstream end of the FRC is compressed, so that assuming a very large value would imply a very small region over which the compression field acts, allowing the front end to remain at large x_s. FRCs with higher elongation are thus preferred. While this might maximize coupling efficiency, it could lead to an extremely long accelerator to achieve the desired Isp. A balance must be achieved. The target x_s is consistent with the MAP experiments and sufficient isolation. It is also consistent with the experiments on the Inductive Plasma Accelerator[10]. This experiment was initiated to study the merging and compression of supersonic FRCs. The accelerator was designed based on the results from MAP. Dynamic formation was employed and downstream x_s values were in some cases even higher than 0.83.

With the ratio of 0.5 and the empirical value of trapped flux expressed in Eq. (9) the target vacuum field can be determined to be $B_{vac} = 0.1$ T. It is noteworthy that there is no explicit size scaling in Eq. (10). That is not to say that one is free to choose the scale arbitrarily. There are several other constraints that will ultimately determine the optimum size. A short list would include the kinetic energy desired per pulse, and the target Isp. In addition there are the constraints imposed by the PPU technology, in particular the maximum coil voltage V_c. The FRC itself imposes constraints due to both confinement and stability issues. The consequences of these constraints will now be considered, with the result being the determination of the prototype thruster operational parameters and dimensions.

The desire to operate at thrust ranges of several hundred Newtons and up to 10 MW, together with Eq. (9) will determine the volume of the MAP thruster. From circuit considerations, both the switching speed of the solid state devices, and the speed at which the local storage capacitance can be recharged determine the rep rate. From previous work on switched power, 20 kHz is a reasonable maximum rate for pulsing the coils. This leaves sufficient time (~ 50 μsec) to recharge the local storage capacitors and fill the source region with propellant for the next pulse. This rate implies that there must be 500 J of directed energy imparted to the plasmoid formed with each pulse to produce 10 MW of directed thrust.

It can be seen that Eq. (10) describes the energy coupling between the coil magnetic energy and the jet energy, with the coupling coefficient determined by the vacuum field (0.1 T) and Eq. (9). The result can be stated as:

$$KE = 500\,J = \frac{\sqrt{2}}{\pi}\frac{0.05}{0.1}E_B \Rightarrow E_B \sim 2\ kJ \tag{15}$$

This in turn imposes a constraint on the thruster volume (radius and length):

$$\frac{2\mu_0}{\pi}\frac{E_B}{B_{vac}^2} = r_c^2 l_{ac} = 0.16 \quad m^3. \tag{16}$$

The target Isp constrains the thruster length. This comes about through the need to have the magnetic field of each coil swing from its minimum to its maximum during the FRC passage in order to maintain the maximum field gradient across the FRC. This is essentially a requirement on the coil voltage since

$$\frac{\Delta B_z}{\Delta z} \sim \frac{dB_z}{dt}\frac{dt}{dz} = const \Rightarrow V_{coil} \sim v_z \tag{17}$$

From Faraday's law one has

$$V = \omega AB = \frac{\pi^2 r_c^2}{2\tau_{1/4}}B = \frac{\pi^2 r_c^2}{l_s}B v_z \tag{18}$$

where it was assumed that the FRC velocity, v_z was such that the FRC moved its length in the half cycle time of the magnetic field. This condition would be most restrictive at the end of the accelerator where the FRC velocity is near its maximum (a target value ~ $6x10^4$ m/s will be assumed). As will be detailed later, a comfortable maximum voltage for a bi-fed, split coil driven by a set of high current solid state switches (IGBTs) anticipated to be used for this purpose is ~ 3 kV. Eq. (18) then implies

$$\frac{V}{\pi^2 B v_z} = \frac{r_c^2}{l_s} = 0.05 \quad m. \tag{19}$$

From Eqs. (17) and (19), eliminating the coil radius as a variable, one finds that the accelerator length should be on the order of at least 3 FRC lengths to reach 500 J of kinetic energy. The ratio of the FRC length to coil radius is controlled by the initial inventory in dynamic formation. Conservatism dictates that the value should be no less than the minimum that has traditionally been employed on past FRC experiments. This is typically around 3. From Eq. (19) one has then

$$r_c = 0.05\cdot(3) = 0.15\ m \tag{20a}$$

$$l_{ac} = (3)\cdot l_s \sim 10\ r_c = 1.5\ m \tag{20b}$$

These values are somewhat larger than what was employed on the initial MAP thruster, but the ratio is similar. This is consistent with the much lower voltage that can be obtained with solid-state switching. The size increase is much less than what would be required if the same very high Isp were to be obtained. The lower voltage, larger thruster is easier to construct as well.

As a consistency check, a 2D MHD calculation was performed with the parameters determined above. It was assumed that the propellant was Argon (A_i = 40) at 1.5 mTorr. This is roughly the same mass density used in the MAP experiments in Deuterium (A_i = 2) at 20 mTorr. Since the size of the thruster is much larger, the actual plasmoid mass is significantly more. It was decided to test with a somewhat larger thruster radius. The reason was based mainly on the fact that radiation, flux, and particle loss may be higher for a potentially higher Z propellant like Argon. Both are reduced by increasing the scale at constant mass (particle) inventory. The coil radius was thus increased 0.2 m. The thruster length was not increased as the coil voltage was kept below 3 kV (2.5 kV).

The results from a non-optimized calculation are shown in Fig. 6. There was no attempt to improve on the coil timing for acceleration. A more uniform acceleration is desirable, and can usually be achieved with different coil

timing, as well as possibly a different starting mass inventory. The point to be made here is that it was possible to achieve the desired range of Isp and mass required, even without an optimization.

Initial results from the RMF startup experiments on ELF indicate that Argon FRCs can be generated. The confinement is still an unknown. Other gases, such as nitrogen N_2, or stoichiometric ratios of ammonia, NH_3, or hydrazine, N_2H_4 could be easily used as well. The latter two have obvious advantages for propellant storage, and is one of the attractive features of an electrodeless thruster.

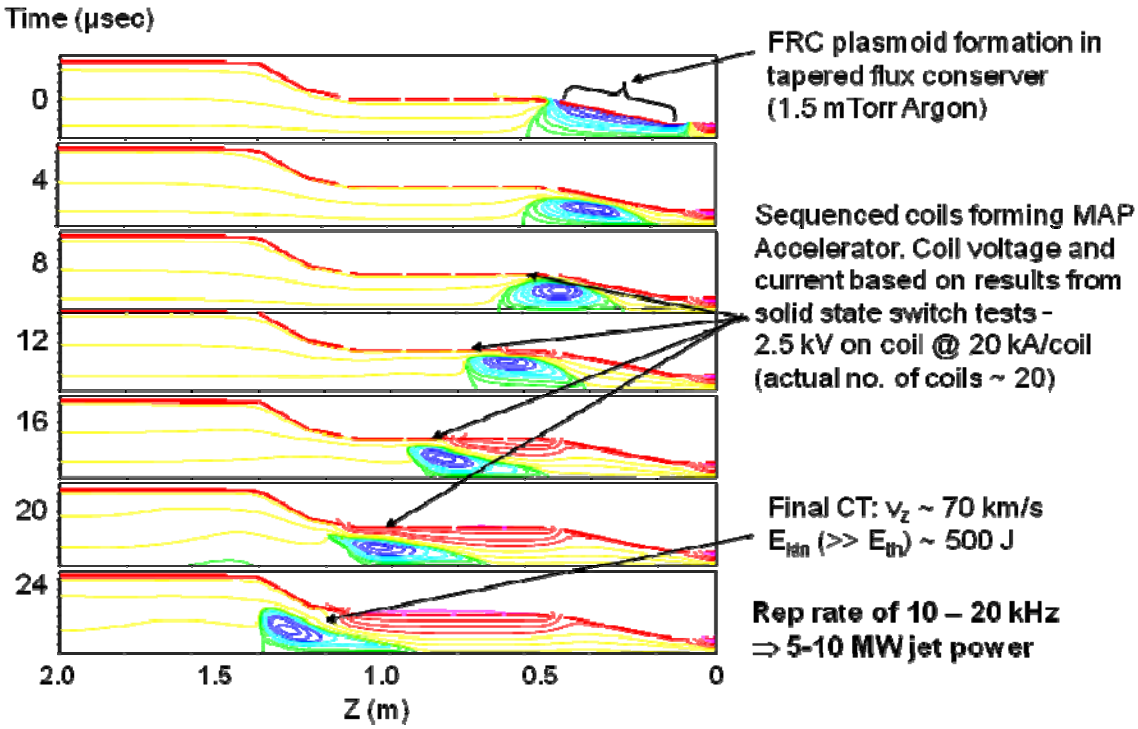

Figure 6. 2D MHD calculation in Argon with RMF startup. *The fill pressure was 1.5 mTorr. Coil voltages were limited to 2.5 kV or less. The calculation starts with field reversal at 5 μsec. field swing was ±*

B. MAP thruster Efficiency

With the main thruster parameters determined, one can now perform an analysis of the potential thruster efficiency. The jet power (energy) is related to the power (energy) source as

$$P_{jet} = \eta_{tot} \cdot P_s \tag{21}$$

The total efficiency can actually be broken down into two components:

$$\eta_{tot} = \eta_{th} \cdot \eta_{ee} \tag{22}$$

where η_{th} is the efficiency of converting the delivered thruster electrical energy into propellant directed energy and η_{ee} is the efficiency of converting source electrical power into delivered thruster electrical power, For the thruster efficiency, η_{th}, a significant loss channel is the energy cost to ionize the propellant. This is true of all thrusters, and MAP is no exception. The energy loss is a function of the atomic or molecular species as well as the electron density and temperature. A commonly used gas in FRC experiments, and the one used in the initial MAP experiments is Deuterium. There are additional penalties for molecular gasses such as hydrogen due to the energy loss from

dissociation. It can actually get much worse as there is usually an additional radiative loss from the atomic excited states during the ionization process. The radiative losses can completely dominate the losses as the atomic mass or electron temperature decreases. For the typical low electron temperature plasmas (~ 3 eV) one finds that in a high mass gas, the energy loss associated with ionization can exceed 40 eV. This additional loss is a sensitive function of both electron temperature and density. Increasing the electron temperature enhances the chance that a electron-neutral collision is an ionizing one (peak cross section ~ 50–80 eV). Increasing the plasma density depopulates the excited state bound electrons thereby reducing radiative losses directly. One advantage of the high densities (~ 10^{21} m^{-3}) and electron temperatures (50-100 eV) obtained in the FRC is that it lowers the ionization losses to essentially that required for ionization.

It would appear that there are far better species for propellant use than what are typically used. Several of the better candidates are liquids or solids. The ability to use these propellants can be a tremendous advantage as it radically simplifies propellant storage. One serious drawback for light gasses such as H and He is the tankage mass which can exceed the propellant mass. The advantages for low atomic mass come from primarily the near absence of additional radiation and second ionization losses that occur with higher atomic number.

There is one propellant that fits into all categories of ideal propellant, i.e. low atomic number, low ionization energy, and a solid at room temperature. This is Lithium. It also has a very low vaporization temperature. Needless to say, several thrusters have taken advantage of this element with the MPD actually having considerable success with it. Lithium has a very low first ionization energy and a very large second ionization energy which is ideal for minimizing the radiation loss. It would also be a highly desirable propellant for MAP. One great advantage of an electrodeless thruster is the ability to essentially work with any substance that can be ionized in some way. It would be advantageous if the MAP thruster could be fueled by a range of propellant masses. Cesium, Uranium, Boron and Beryllium would allow for a wide range in propellant mass for a given electron density. The question would be how to produce such plasmas. Such a possibility may exist in the form of laser ablation.

Laser produced plasmas provide an intriguing method for loading particles into a FRC plasmoid to attain both high mass density and high pulse rate operation. Laser produced plasmas could be the actual ion/electron pair source that is created inside the FRC magnetic field for an almost instantaneous increase in current drive. With a laser based initiation of the discharge, combined with propagating wave acceleration, the plasma propellant would have no contact with the thruster throughout the entire process. There would be no need of any electroded assist even for breakdown/preionization. It would eliminate the need for gas storage and handling as well as the systems required for fast gas puffing or metering. It would also provide for a means to operate the device with any material substance - solid or liquid. This would open the thruster window of operation to a host of propellants that have never been accessible to electric propulsion before. This mode of operation could offer the highest efficiency and provide for the least power flow back on to the thruster. MSNW is currently looking into the feasibility of testing this approach. For the discussion here, it will be assumed that Lithium is the propellant to be employed in the MAP thruster.

If ionization losses were the only energy cost in the production and acceleration of the FRC plasmoid, the ideal MAP thruster would have an efficiency of

$$\eta_{th} = \frac{E_d}{E_d + E_i + E_{Loss}} \tag{23}$$

where E_d is the directed energy, and E_i is the energy loss associated with ionization. All thrusters will have these elements in common. For most thrusters, there are additional energy loss terms, E_{Loss}. A short list would include

(1) Electrode (boundary) voltage (sheath) drops - E_{sh}
(2) Thermal transport to the thruster body - E_{cond}
(3) Unconverted thermal energy at ejection (frozen flow loss) E_{ff}
(4) Radiation from plasma – E_{rad}
(5) Convective plasma loss to thruster E_{conv}.

For the electrodeless MAP thruster, (1) and (2) are not important. The CT is well adapted to the use of a magnetic nozzle for excellent thermal conversion so that (3) is also a minor loss. The radiation issue could be important if a propellant mass beyond lithium is employed. The RMF initiated plasmoid helps avoid this problem and allows for much higher masses. The importance of this can be seen from the Eq. (23). The surest way to increase the thrust efficiency is to increase the directed energy of the propellant. This means either increased mass or velocity. If there is an optimum velocity for the mission, it means increased mass. Electrodeless RMF formation should allow for CT thruster efficiencies as high as ion thrusters.

Given that there are at least three distinct modes in which in may be possible to operate the MAP thruster, not to mention various propellants, the best course at this point is to try to evaluate the appropriate range operation and propellant choice for the target Isp (6 ksec) and power (10 MW), and estimate the magnitude of the directed energy expected as well as the losses from the list of loss channels previously mentioned. The best guide will be the results of the numerical modeling for most of the values. This is essentially what has been done for both the PIT and MPD thrusters as it is quite difficult to extract an independent measure of these quantities experimentally. Several of these loss channels would require detailed global measurements. In addition, the losses experienced experimentally are quite often due to operational constraints far from ideal due to budget and time limitations. These problems would most likely not be present in the actual thruster operation.

A good case in point is the MPD thruster. Steady operation at high electrode temperature has consistently demonstrated much better thruster performance with less electrode erosion, sheath losses, and frozen flow losses than quasi-steady pulsed operation of the thruster. Similar changes in behavior should be expected for the MAP thruster as well. The estimation of the magnitude of the losses must be considered in this light. The values shown in Table 1 were evaluated by considering the intrinsic behavior of the plasma based on previous experience with many similar types of plasma that have been studied in greater depth.

Table 1. MAP Thruster Energy Flow for Different Modes and Propellants

MAP Mode	E_d (J)	E_i (J)	E_{cond} (J)	E_{ff} (J)	E_{rad} (J)	E_{conv} (J)
RMF –D	500	100	0	20	10	20
RMF – Li	500	25	0	15	10	25
RMF – Ar	500	15	0	15	20	50

MAP Mode	η_{th}	I_{sp} (ksec)	$^{*}T$ (N)	$^{\#}P_{jet}$ (MW)	ε_B	$^{+}\eta_{ee}$
RMF –D	0.77	10	200	10	0.3	0.83
RMF – Li	0.87	8	250	10	0.35	0.86
RMF – Ar	0.83	6.7	300	10	0.35	0.86

$^{\#}$ Jet power is adjusted to be 10 MW by the rep rate (20 kHz).
* Thrust is calculated based on the20 kHz rep rate needed to provide 10 MW jet power.
$^{+}$ effective electrical efficiency is calculated according to Eq. 24 assuming a 5% resistive loss in PPU for all devices.

The values for the RMF mode are based on both the experimental results as well as the Moqui 2D MHD numerical calculations. As an illustration of how the numbers in the table were derived, one considers the first line calculations for the RMF MAP thruster in Deuterium. From the MOQUI calculations the post nozzle directed CT energy was 0.49 kJ. The particle inventory was 0.1 mg/3.2x10^{-21} (mass of D ion) = 3.1x10^{19} ions. The preionization energy loss is not much greater than the ionization and dissociation energy. As pointed out earlier, this is minimized at the high electron temperature and density achieved for this mode in Deuterium, so that FRC formation is about as efficient as one can get in this regard. A good number is 20 eV per ionization so that E_i is 100 J.

With conventional plasmoid formation, the plasma is in contact with the tube wall during the field reversal. The time of contact is roughly 200 ns. Given the tube size and a sheath temperature ~ 10 eV from prior 1D numerical modeling, a 5 eV per electron energy loss can be ascribed to thermal conduction during this time. With RMF plasmoid formation there is no reversal. In fact there is a general inward plasma flow essentially eliminating particle loss as well[5]. One can assume 2 eV of radiation loss during the residence time in the thruster based on equilibrium radiation loss rates observed in other FRC experiments. It is very likely that this is also an unnecessary loss as repetitive operation will most likely reduce the impurity content of the FRC. The initial FRC reflects contaminants

adhered to the wall and entrained in the FRC at reversal. Subsequent pulses will contain less and less as time goes on.

The frozen flow loss was 20 J in the 2D MHD calculation. The particle loss observed was most likely numerical as the adaptive grid movement at supersonic velocity has this consequence. FRC translation experiments indicate negligible particle loss during translation. A reasonable value would be to assume that the loss is as large as the mean value between the loss rate observed during *in situ* experiments in the source coil and in the translation chamber. This would imply that roughly 2.5% of the FRC inventory is lost to the upstream boundary. It is assumed that the particles are lost at the average velocity acquired during acceleration. This leads to a convective loss of 20 J. The losses then total to 150 J. The thrust efficiency would thus be ~ 77% for RMF startup with the D_2 propellant. It desirable to lower the Isp for most near earth orbit maneuvering. Lithium lowers the Isp as well as the ionization losses, and provides for greater thrust for a given power input as the table indicates. The efficiency should always be high as long as one can avoid significant radiation losses. With higher mass propellants, both the lower densities and short time from formation to ejection will help considerably as there will be little enough time to populate higher ionization states and energy levels.

A column in the efficiency table contains a quantity that is labeled ε_B, and represents the coupling coefficient between the energy flow into the magnet system to dynamically form and accelerate the plasmoid, and the energy delivered to the load. The load in this case is the energy in the form of energy flow into the plasma system, i.e. $E_d+E_i+E_{Loss}$. It is this term that measures how efficiently the energy from the PPU can be utilized. It is NOT the efficiency of the thruster or the PPU. It could be compared to the ballast resistor in the typical arcjet or MPD load matching resistor. In these cases the energy that was not coupled into the discharge was lost to the system in the form of heat. These losses are not usually considered part of the thruster loss as they would never be employed in the actual thruster implementation for space.

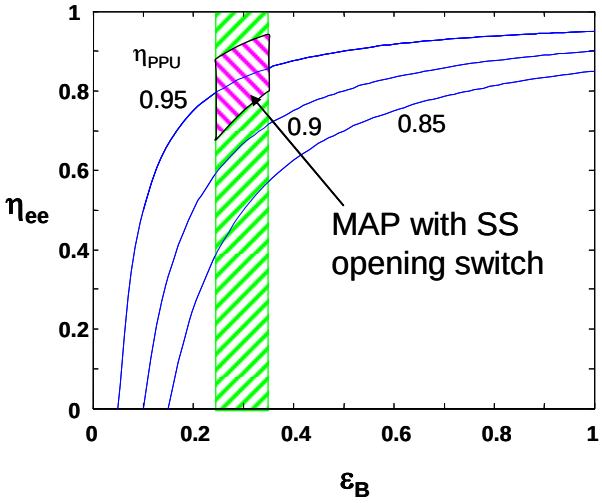

Figure 7. The overall electrical efficiency, η_{ee} as a function of the magnetic energy coupling coefficient ε_B for various PPU efficiencies. *The green shaded region represents the range of coupling observed in past FRC acceleration experiments.*

For purely electromagnetic coupling as in the MAP thruster, it is a bit different. Except for what is transferred to the plasma, the energy flow here is virtually all reactive. Energy flows into the magnet only to flow back into the capacitor minus some resistive loss in the conductors, cables and switches. In the usual FRC formation scenario using spark gap or ignitron switching, the entire stored energy is lost resistively by "crowbarring" the current so that it circulates through the magnet until all of the magnetic energy is dissipated in the switches, cables, and conductors. This does not need to happen any more than it is necessary to lose virtually all of the energy in a ballast resistor. To avoid the energy loss one could continue to oscillate the coil current producing a new plasmoid on every half cycle as was done in the initial MAP experiments. This however led to a very high power thruster. To reduce the power an opening switch must be employed to inhibit the flow of energy after the FRC has passed through that coil, reserving it for the next pulse. It is has been difficult if not impossible to do this in prior experiments, as repetitive pulsing was not a priority. These circuit losses however have nothing to do with either the thruster efficiency or that of the ultimate PPU, and will be avoided in the modifications planned for the new MAP thruster.

That being said, there is some significance to the coupling coefficient. With the transfer of energy not being 100%, the overall PPU efficiency is reduced. For the sake of argument let us say that the coupling efficiency is ~30% (similar to what it is estimated for a MAP thruster). This means that roughly three times as much energy must be circulated into the magnets to transfer a given energy. If the resistive losses in the PPU (switches, cables, and coils) were 3% of the energy transferred ($\eta_{PPU} = 0.97$), the effective electrical efficiency, η_{ee}, would be:

$$\eta_{ee} = \left(1 - \frac{1-\eta_{PPU}}{\varepsilon_B}\right) \quad = \quad 0.90. \tag{24}$$

The PPU efficiency is thus reduced by poor coupling efficiency. This can be seen graphically in Fig. 7. It is important that the coupling be greater than ~30% to avoid the necessity of needing an extremely high PPU efficiency.

Efficient energy transfer to the plasma is assured by the electromagnetic interaction. With RMF plasmoid initiation, the entire process of formation, acceleration and ejection can be accomplished with essentially no contact with the thruster body. The circuit losses do not have to be high as there is nothing being done here that isn't accomplished in industrial lighting or electric switched transmission where efficiencies are 95-98%. The difference is the magnitude of the power transfer and the compact nature of the load. Transmission and coil losses can be made minor by the use of the appropriate conductor geometry (i.e. multi-filar windings) and the appropriate switch technology (i.e. solid state). There is a strong need to develop these technologies for the MAP thrusters, just as in the case of the MPD thruster for high power. There must be a focus on both the physics and the technology as both are needed for success.

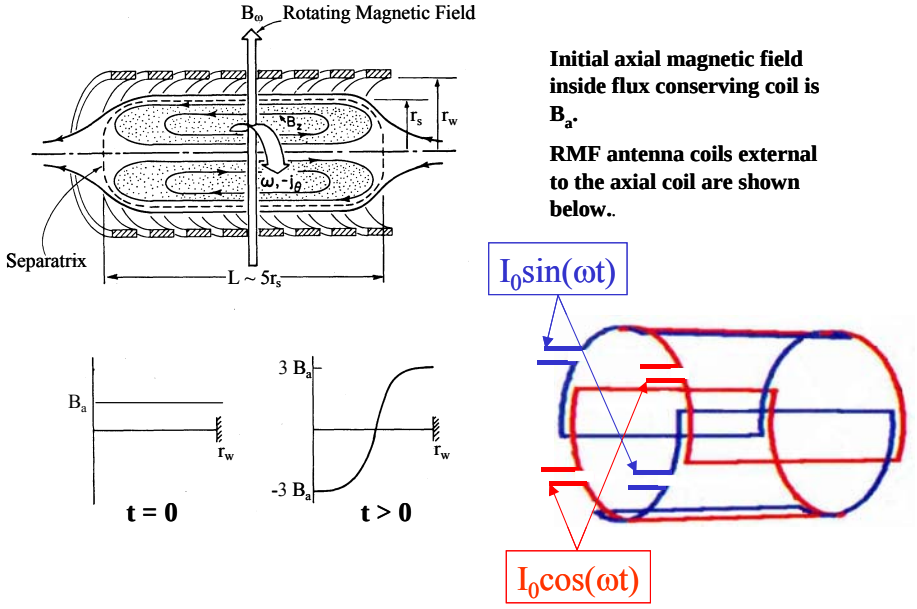

Figure 8. RMF antenna and current drive in a solenoidal, flux conserving coil.

III. New MAP Thruster

A. FRC Plasmoid Generation Employing a Rotating Magnetic Field

The MAP thruster no doubt represents one of the highest power electric thrusters and possibly the best approach to a multi-megawatt thruster, but it currently relies on an inductive startup requiring high voltage pulsed power. The formation of the FRC plasmoid also incorporates a brief plasma interaction with the thruster wall during the rapid field reversal. Both of these detractions can be eliminated, and the efficiency of plasmoid formation significantly improved by the generation of the required plasma current by the rotating magnetic field (RMF) technique. An illustration of the magnetic field structure of the RMF generated FRC is found in Fig. 8. The FRC plasmoid is formed in a constant axial magnetic field by the pair of RF oscillator antennas positioned radially outside the axial field coils. These antenna pairs form the two orthogonal magnetic field components required to produce the rotating magnetic field when phased 90° apart.

The direction of rotation of the RMF is such as to generate an azimuthal diamagnetic current that produces a radially inward confining force on the plasma. With a sufficiently large azimuthal current, the plasma is completely confined by the closed magnetic field generated by the plasma currents. In this manner the RMF provides for both a contact and electrode free FRC plasmoid formation.

The experimental RMF configuration that was used to establish the use of RMF for plasma generation at high density was the STX-HF experiment (STart-up eXperiment at High Field) at the University of Washington (UW)[9]. The attainment of high field and power in a geometry for propulsion was finally achieved in the results on the Electrodeless Lorentz Force Thruster (ELF)[8]. Here the initial drive and confinement of the plasmoid was changed from a constant radius coil to that of a tapered conical coil like that depicted in Fig. 9.

A starting point for understanding the current drive process is the generalized Ohm's Law, where it will be assumed for the moment that the ions form a fixed uniform background and the **u×B** term can be ignored:

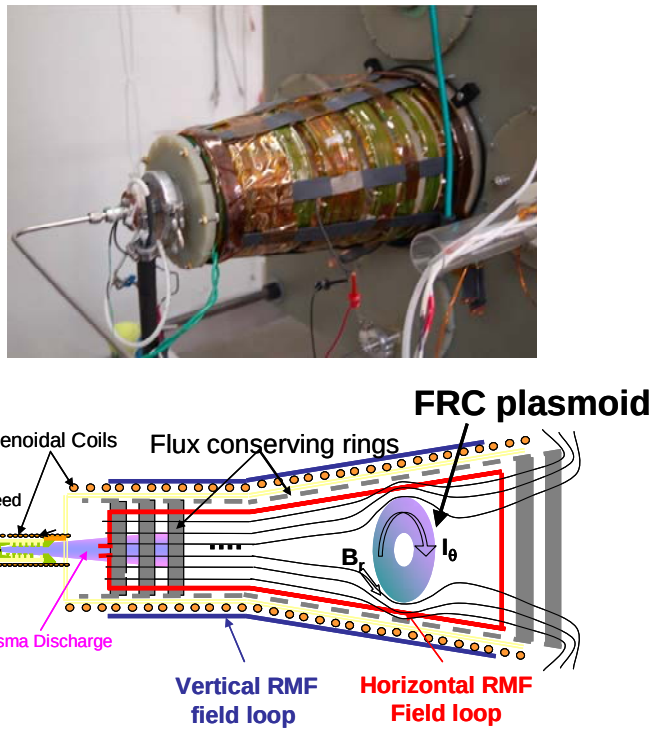

Figure 9. MAP Thruster RMF startup configuration. *Top: Picture of the device constructed for testing. Bottom: schematic showing operation.*

$$\mathbf{E}+(\mathbf{u}\times\mathbf{B}) = \eta\mathbf{j}+\mathbf{j}\times\mathbf{B}/ne \quad \Rightarrow \quad \mathbf{E} = \eta[\mathbf{j}+(\omega_{ce}/\nu_{ei})\mathbf{j}\times\mathbf{e_B}] \tag{25}$$

where B has oscillating components in the θ and r directions due to the RMF at a frequency ω_{RMF}, and a steady axial field provided by the axial field coils. If the Hall term $\mathbf{j}\times\mathbf{B}/ne$ is small compared to the resistive term, $E_\theta = \eta j_\theta$ is positive, and from Faraday's law, $d\phi/dt$ is negative and the plasmoid configuration decays. With the Hall term dominant, E_θ, for sufficiently small η or large $\langle j_z B_r\rangle$, can be negative with a subsequent increase in flux and a growing magnetized plasmoid configuration.

The solution of Ohm's law, neglecting the Hall term, is characterized by the RMF penetrating a distance $\delta = (2\eta/\omega_{RMF}\mu_o)^{1/2}$, the resistive skin depth for an RF field in a conductor. However, the regime of interest here is a plasma where $\nu_{ei} << \omega_{ce}$. In this limit, from Ohm's law, $j_\theta \approx -ne\eta\omega_{RMF}$ and $j_z \approx E_z/(\eta\omega_{ce}^2/2\nu_{ei}^2)$. The electrons are in synchronous rotation with the RMF and their response to the axial electric field of the RMF antenna is severely restricted (small j_z), and unable to screen out the RMF field. From another viewpoint, the co-rotating electrons experience a nearly steady transverse field, and the effective field penetration can be many times the resistive skin depth. The Hall term has a pondermotive component, the $\langle j_z B_r\rangle$ term, acting in the θ direction. Since j_z, B_r, and B_θ vary in time at the frequency ω_{RMF}, the pondermotive force in the θ direction has a steady part and an oscillatory part at a frequency of $2\omega_{RMF}$. From the steady $\langle j_z B_r\rangle$ force, the electron fluid attains a steady value of azimuthal velocity, $v_{e\theta}$ that corresponds to the balancing of the steady accelerating torque by the retarding torque (due to the collisions of the electrons with the ions). In this way a steady azimuthal current density,

$$j_\theta = -n(r)\,e\,\omega_{RMF}\,r \tag{26}$$

is produced. With the current profile determined by Eq. (26), the magnetic field profile is also specified. The resultant profile is the RR profile due to the constant angular drift velocity of the electrons produced by the RMF. With the RR profile, the axial confining field produced by the current is given by

$$B_e \cong 0.2\,\mu_0\, e\, n_0\, \omega_{RMF}\, r_s^2 \tag{27}$$

Eq. (27) can thus be used to determine the RMF frequency required to provide for the necessary accelerating magnetic field. For the initial ELF experiments, $\omega_{RMF} = 1.5\text{x}10^6$, or a frequency of 235 kHz, and a field $B_e = 1.4$ kG was produced at the thruster exit. This is a record for RMF and provides for a sufficiently high field to assure a strong axial JxB force for rapid ejection even in Argon. The peak plasma density inferred from these results and Eq. (27) was $2.5\text{x}10^{20}$ m^{-3}, also a record.

The antenna driver that was employed in the ELF experiments was produced by simple resonant circuits employing solid state IGBT switches. The circuit power loading for these experiments was determined by the phase shift between the current and antenna voltage, as well as SPICE modeling. The final maximum power that the thruster was tested had a peak loading of 1.6 MW. It was not possible to maintain the power at this level for vary long as the power supply capacitors continually discharge to lower voltage. To maintain this power would require a very large bank. This is certainly possible and would be done in the prototype system now under construction.

B. Initial Coil Design and Circuitry

The main consideration when it comes to the design of the coil driver circuit is the maximization of the coil voltage. The essentially sets the rate at which energy can be added to the thruster, as well as the maximum Isp as described above. Fortunately the relatively lower values of Isp needed for most missions such as rapid orbit maneuvers bring the required voltages down to the range of the solid state switches that are easily obtained. From Eq. (19) it can be seen that with a larger the voltage, not only can one attain a higher Isp at constant size, but one could also increase B and hence propellant mass. It can also be seen from this equation that higher voltage would also allow for a larger (lower density) thruster, or a shorter one with lower transport losses. The limitation is the voltage that can be achieved with the use of solid state switching. At first glance, this does not seem to be a significant issue. Voltages as large as 4 kV have been achieved with single devices that can operate at the high speed required here. The problems stem from the massive parallelization required due to the low impedance nature of the MAP accelerator coils. With the basic coil parameters determined one can evaluate this impedance for the prototype rep rated thruster:

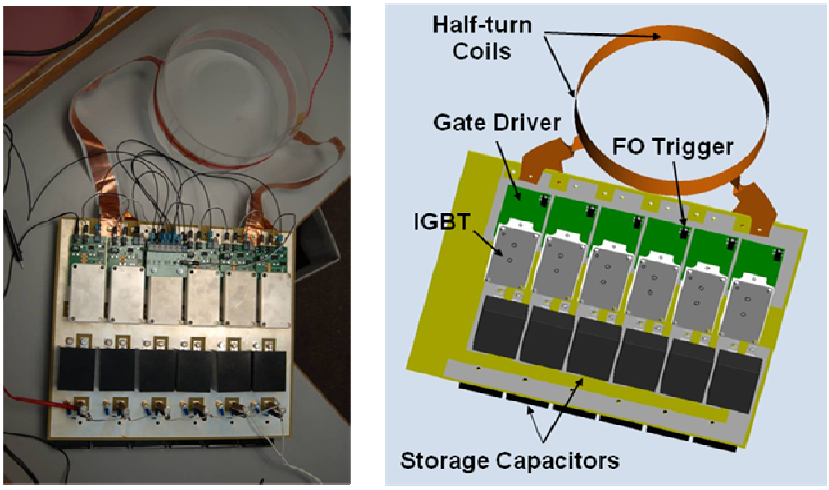

Figure 10. Solid state driver and power supply for a single bi-fed coil on the MAP accelerator

$$Z = \omega L = \frac{\pi v_z}{l_s}\frac{\mu_0 \pi r_c^2}{l_{ac}} K_L \cong 0.02 \tag{25}$$

where κ_L is the correction coefficient for a finite length coil and is roughly = 0.88 for the aspect ratio determined for the MAP thruster. The peak current flow for a coil voltage of 3 kV is thus 150 kA. This is a substantial current and demands that the high current class of solid state switches (IGBTs) be employed.

Considerable experience has been gained in the use of the Semikron "brick" style devices which can switch up to 2 kA per device in a pulsed mode. The current per unit length required is roughly 1 kA/cm to achieve the target B_{vac} = 0.1 T. The prototype driver module consists of a set of 6 such IGBTs mounted to a large PC board along with the snubbers, triggers, and local energy storage capacitors. A schematic as well as a photograph of a coil driver module is shown in Fig. 10. The conduction layers on the board are manufactured out of silver in an extra thick layer to handle the large current flows. Each module will nominally provide 10-15 kA. The result from testing at a voltage and current in excess of what is required is shown in Fig. 11. The device was operated for several pulses in a burst mode at 20 kHz. It was not possible to operate for longer due to power supply limitations. This was sufficient however to demonstrate adequate energy recovery back onto the capacitor with no plasma load. Further improvement is expected with a shorter stripline and thicker, lower resistance coil. A stripline feed off the leading edge of the module will directly feed each coil of the MAP thruster in the prototype.

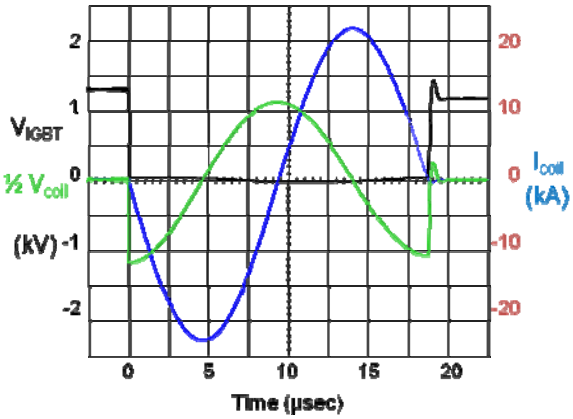

Figure 11. Module performance for device depicted in Fig. 8 (single pulse) at 1.3 kV charge.

In order to develop the high voltage required, a novel circuit has been designed to provide for as large a voltage as needed, and that is still compatible with the 1700 V limit of the individual IGBTs. A series arrangement of the IGBTs would provide a means to increase the voltage to the coil. There are several very good reasons why this approach was not taken. The most significant problem with the series arrangement is the prefire of any of the devices. This switch closure can occur for many different reasons such as noise on the gate, an incorrect timing of the switch closure, or a failure of the device itself. The consequence however is the same for all of them – the voltage appears across all of the other solid state switches destroying them. This is the one liability of solid state switching. The switches are intolerant of overvoltage. This however is more than compensated by their much higher efficiency in switching, and of course their ability to be opened and closed repeatedly without wear or erosion. Fortunately, there is a method where the switches can be operated in a manner that generates a large loop voltage as required. In its simplest configuration, it has been given the name "bi-fed half-turn coil" in an attempt to describe how it looks and operates. It is illustrated in Fig. 12. In order to double the voltage on the coil without doubling the charge voltage, it is necessary to split the coil into two halves. The key to doubling the voltage without incurring a large stray inductance penalty is to have each coil half driven by the same module. Stripline from each module must run to both coil feed points. The polarity of one of the two cables is reversed so that the voltage on the coil is doubled. The module of course is only at half of this voltage. The current in each half of the magnet is returned on the cable (or stripline) used to feed the other side. For the stripline feed, which is currently the method planned for MAP, the stripline must undergo a 180 degree twist as it traverses to one of the ends (see Fig. 10).

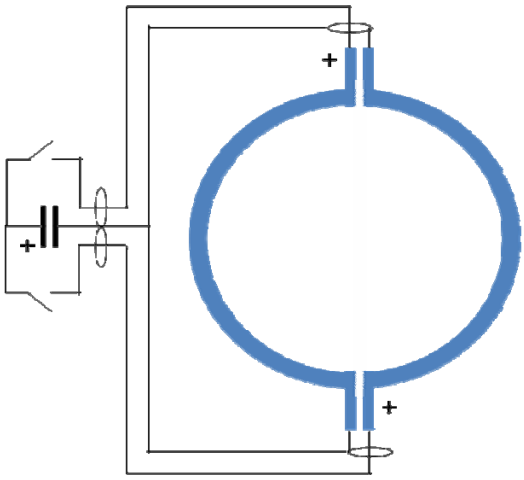

Figure 12. Bi-fed, half-turn coil to be employed on MAP for voltage doubling.

If more voltage were to be desired, the configuration could be changed to a tri-fed third-turn coil, or a quad-fed quarter-turn coil. With the addition of each coil split however, the current that must be provided to each section must be the same if the same flux in the coil is to be the same. This means that each module supply must produce two, three, or four times as much total current. That is actually a preferred scaling as current switching is what IGBTs do best. Even though the number of modules will be doubled for the bi-fed coil to operate at twice the voltage, it is well within the capability planned for the coil drivers. The design therefore calls for two 10 kA modules to be positioned every 10 cm along the length of the MAP thruster. A schematic of the final MAP accelerator is shown in Fig. 10. The modules will be triggered in a sequential manner to produce a travelling magnetic wave with a field swing from trough to peak of up to 0.3 T. This will provide for operation up to 1.5 kJ per pulse. By varying the timing the wave speed can be varied to produce a range of final velocities from 50 to 150 km/sec.

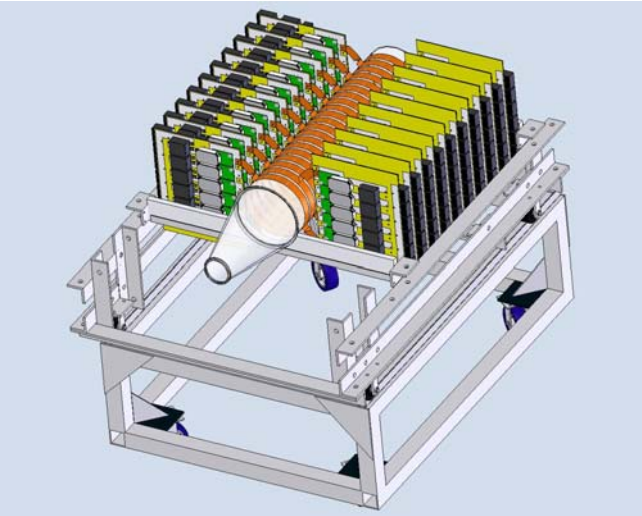

Figure 10. Full assembly of modules for MAP accelerator. *The coils and RMF antenna have been removed from conical source tube for clarity.*

IV. Conclusion

The production of field reversed configuration (FRC) plasmoid and subsequent acceleration by magnetic forces is a promising approach to high-thrust and high performance space propulsion. A research facility was designed to demonstrate this potential, determine optimal performance, and examine the technology required to move toward the design of practical high-performance space propulsion system. This facility has been constructed, and preliminary results have been obtained. The Magnetically Accelerated Plasmoid (MAP) thruster in its initial operation produced plasmoids at very high Isp (18-20 ksec) and demonstrated operation at very high peak power (70 MW). An analysis for optimizing the thruster to operate at high efficiency at lower power and Isp (10 MW and 6-8 ksec) was carried out. Estimates of all the possible energy loss channels for the new thruster configuration were made for a range of propellants with the expected efficiency for the new MAP thruster in the range of 70 – 80%. A method for producing a FRC plasmoid relevant to the new MAP thruster startup using a rotating magnetic field was developed. The design and testing of the solid state power modulation system needed for repetitive operation was accomplished. The full implementation of both the RMF startup and MAP accelerator are the near term goals of the experimental research.

Acknowledgments

This research is supported by the United States Air Force Research Laboratory, Edwards Air Force Base.

References

[1]M. Tuszewski, "Field Reversed Configurations", *Nuclear Fusion* Vol. 28**,** 1988 pp. 2033

[2]John Slough, "Multi-Megawatt Propulsion Based On A Compact Toroid Thruster", IEPC-2005-296, *The 29th International Electric Propulsion Conference, Princeton University, October 31 – November 4, 2005.*

[3]John Slough and George Votroubek, "Magnetically Accelerated Plasmoid (MAP) Propulsion", AIAA2006-4654, 42nd AIAA/ASME/SAE/ASEE Joint Propulsion Conference and Exhibit, 9 - 12 July 2006, Sacramento, CA.

[4]J.T. Slough, "Megawatt Plasma Thruster Based On An Inductive Plasma Accelerator (IMPAC)", Space Technology and Applications International Forum, Albuquerque, NM, January, 2000.

[5]Slough, J.T. and Miller, K.E., "Enhanced Confinement and Stability of a Field Reversed Configuration with Rotating Magnetic Field current drive", *Phys. Rev. Lett*. **85** 1444 (2000)

[6]E.Y. Choueiri and J.K. Ziemer, "Quasi-Steady Magnetoplasmadynamic Thruster Database", *Journal of Propulsion and Power,* Vol. 17, No. 5, 2001, pp. 9673.
[7]C.L. Dailey and R.H. Lovberg, *The PIT MkV pulsed inductive thruster*, Technical Report NASA CR-191155, TRW Systems Group, July 1993.
[8]John Slough, "Electrodeless Lorentz Force Thruster for High Power Propulsion", Final Technical Report, Defense Technical Information Center, Belvoir, VA.
[9]Slough, J.T., and Andreason, S.P. "High field RMF FRC experiments on STX-HF", Submitted to *Physics of Plasmas*.
[10]G. Votroubek, J. Slough, S. Andreason, and C. Pihl, "Formation of a Stable Field Reversed Configuration through Merging" *Journal of Fusion Energy*, (to be published 2007).